Tropical Journal of Drug Research September 2025; 2 (9): 231 - 244
ISSN: 2476-8065 (Electronic)
Available online at http://www.tjdr.org
https://doi.org/10.26538/tjdr/v2i9.3

Original Research Article

In-vitro, Bioinformatics and Computational Biophysical Analyses of Antifungal Phytochemicals from *Acalypha wilkesiana* Variants Targeting Malassezia Lipase

Okechukwu K. Nwofor[1], Chidi E. Duru[2*], Chioma N. Nwofor[3]

[1]*Department of Physics, Imo State University, Owerri, Nigeria*
[2]*Theoretical and Computational Chemistry Research Group, Department of Chemistry, Imo State University, Owerri, Nigeria*
[3]*Department of Microbiology, Imo State University, Owerri, Nigeria*
*For correspondence: Email: chidiedbertduru@gmail.com, +2348037131739

Sent for review: 11 August 2025 Revised accepted: 23 September 2025

Abstract

Purpose: Seborrheic dermatitis (SD) is a common chronic inflammatory skin disorder, often associated with the activity of lipid-hydrolyzing enzymes secreted by *Malassezia globosa*. Conventional antifungals often show limited efficacy and adverse effects, while the mechanisms underlying traditional remedies like *Acalypha wilkesiana* remain underexplored.
Methods: This study evaluated the antifungal potential of phytochemicals derived from the red and green variants of *A. wikesiana*, targeting *M. globosa* lipase (PDB ID: 3UUE). Crude ethanol extracts were analyzed via gas chromatography–mass spectrometry (GC-MS), and preliminary in-vitro antifungal activity was assessed against *M. globosa*. Identified compounds were subjected to molecular docking and molecular dynamics (MD) simulations to assess binding affinity and stability. ADMET profiling and density functional theory (DFT) calculations were employed to predict pharmacokinetics, toxicity, and electronic reactivity.
Results: The red *A. wikesiana* extract demonstrated strong antifungal activity, producing a 60 mm inhibition zone, while the green variant was inactive. Molecular docking identified aspidospermidin-17-ol, 1-acetyl-19,21-epoxy-15,16-dimethoxy- (ASP) as the top-performing compound with a binding affinity of –6.8 kcal/mol, outperforming ketoconazole and the native ligand. MD simulations confirmed the structural stability of the ASP–lipase complex, exhibiting minimal RMSD fluctuations. ADMET predictions indicated low dermal and systemic toxicity, and DFT analysis confirmed favorable electronic properties.
Conclusion: The findings highlight ASP from red *A. wikesiana* as a potent and safe inhibitor of *M. globosa* lipase, supporting its potential development as a novel, plant-based topical antifungal agent for the management of seborrheic dermatitis.

Keywords: Seborrheic dermatitis; *Malassezia globosa*; *Acalypha wikesiana*; Lipase inhibition; Molecular docking

Tropical Journal of Drug Research is indexed by Chemical Abstracts, Embase, Index Copernicus, EBSCO, African Index Medicus, JournalSeek, Directory of Open Access Journals
(DOAJ), African Journal Online, Bioline International, Open-J-Gate and Pharmacy Abstracts

INTRODUCTION

Seborrheic dermatitis (SD) is a prevalent skin condition that primarily affects infants and young adults, manifesting as yellowish, scaly patches in areas with high concentrations of sebaceous glands, such as the face, eyebrows, eyelids, nose, ears, and chest.[1] The early onset in pediatric populations has been linked to heightened sebaceous gland activity, stimulated by maternal

hormones in conjunction with interactions with the cutaneous microbiome.[2] In adolescent and adult populations, seborrheic dermatitis exacerbation has been associated with various factors, including sebaceous gland activity, fungal colonization by *Malassezia* species,[3] and environmental conditions. The *Malassezia* genus, comprising eukaryotic cells, is a natural component of the skin's microbial flora, with lipophilic and lipid-dependent species.[4] This genus encompasses seventeen distinct species, ten of which are well-established on human skin at various sites.[5] Notably, *M. sympodialis* is the most frequently identified and studied species, while *M. pachydermatis* is typically associated with canine skin.[6] In contrast, *M. furfur*, *M. restricta*, and *M. globosa* are commonly observed in diseased human skin, suggesting a potential role in the pathogenesis of seborrheic dermatitis.

M. globosa, a fungal lipase, exhibits strict specificity for mono- and diacylglycerol substrates, although the underlying mechanism remains poorly understood. On healthy skin, it acts as a commensal, but when this relationship is disrupted, the yeast secretes lipases to re-establish itself. These enzymes hydrolyze skin lipids, producing saturated and unsaturated fatty acids, which are either absorbed by the organism or deposited on the stratum corneum, potentially leading to superficial disorders like seborrheic dermatitis (SD).[7] SD has a higher prevalence compared to other diseases like pityriasis versicolor and atopic dermatitis, with approximately 50 million Americans affected and $300 million spent on treatments annually.[8] However, current treatments, including antifungals, keratolytics, and steroid creams, have limitations due to reoccurrence and resistance. Therefore, alternative approaches are necessary, especially for infants with sensitive skin. Medicinal plant extracts have been used worldwide as alternative remedies, and research has demonstrated their efficacy in treating SD.[9] Further investigation into the potential of herbal remedies may provide a valuable adjunct to conventional treatments for SD.

M. globosa, a fungal lipase, exhibits strict specificity for mono- and diacylglycerol substrates, although the underlying mechanism remains poorly understood. On healthy skin, it acts as a commensal; however, when this relationship is disrupted, the yeast secretes lipases to re-establish itself. These enzymes hydrolyze skin lipids, producing saturated and unsaturated fatty acids that are either absorbed by the organism or deposited on the stratum corneum, potentially leading to superficial disorders such as SD.[7] SD has a higher prevalence than other diseases, including pityriasis versicolor and atopic dermatitis, affecting approximately 50 million Americans and accounting for an estimated $300 million in treatment costs annually.[8] Current therapies, including antifungals, keratolytics, and steroid creams are limited by recurrence and resistance. Therefore, alternative approaches are necessary, particularly for infants with sensitive skin. Medicinal plant extracts have been used worldwide as alternative remedies, and research has demonstrated their efficacy in treating SD.[9] Further investigation into the potential of herbal remedies may provide a valuable adjunct to conventional treatments for SD.

Acalypha wikesiana, a member of the Euphorbiaceae family, is a versatile plant species with a rich cultural heritage and diverse applications. Commonly known as copper leaf, fire dragon, or beefsteak plant, it is widely distributed across the tropics of Africa, America, and Asia, having originated from the South Pacific islands. Its ornamental value is attributed to its vibrant, heart-shaped leaves, which display a wide range of colors, including bronze-red, green, yellow, brown, purple, and orange. The leaves, stems, and flowers of *A. wikesiana* have been extensively studied for their phytochemical composition, revealing the presence of alkaloids, glycosides, saponins, phenols, tannins, carbohydrates, crude protein, crude fat, flavonoids, and terpenoids.[10] Moreover, the leaves have been reported to exhibit antifungal activity against various fungal strains, including *Microsporum canis*, *Trichophyton rubrum*, *Aspergillus niger*, *Aspergillus flavus*, *Trichophyton mentagrophytes*, *Candida albicans*, and *Malassezia furfur*.[11-14] The plant's traditional uses such as the treatment of headaches, colds, wounds, and skin infections, have been validated through scientific studies, underscoring its potential as a valuable resource for herbal medicine.

In various regions across Africa, *A. wilkesiana* is found predominantly in red and green foliage variants. Among traditional healing communities, a well-established practice involves the aqueous extraction of *A. wilkesiana* leaves, whereby the foliage is boiled to obtain a decoction that is subsequently used as a therapeutic bath for infants under five years of age.[15] This treatment is traditionally administered to manage cutaneous conditions such as rashes and seborrheic dermatitis. Empirical observations among users report notable improvements in skin health, including rapid resolution of dermatological symptoms and restoration of dermal smoothness within a few days of application. However,

anecdotal discrepancies exist regarding efficacy, with some practitioners favoring the red variant for its presumed superior potency, while others advocate for the green variety.

In this study, advanced computational methods including molecular docking, molecular dynamics simulations, ADMET (Absorption, Distribution, Metabolism, Excretion, and Toxicity) profiling, and density functional theory (DFT) calculations were employed to provide a comprehensive evaluation of the antifungal potential of *A. wilkesiana* phytochemicals. Molecular docking enabled the prediction of binding affinities and interaction profiles between the bioactive compounds and the lipase target of *M. globosa*, while molecular dynamics simulations validated these interactions under near-physiological conditions by assessing the conformational flexibility and stability of the complexes over time. ADMET profiling further complemented these approaches by predicting the safety profile of the lead compounds for topical antifungal application. DFT analyses added another layer of mechanistic insight by characterizing the electronic properties, reactivity indices, and stability of the lead phytochemicals, thereby providing quantum-level validation of the docking and dynamics results. Collectively, these complementary methods ensured a robust, multidimensional assessment of the antifungal efficacy and therapeutic potential of the studied compounds. By combining traditional ethnopharmacological knowledge with modern computational drug discovery strategies, this integrative approach provides a rational foundation for the development of safe, effective, plant-based antifungal therapeutics for the management of seborrheic dermatitis.

MATERIALS AND METHODS

Collection and isolation of *M. globosa* inoculum

A well-characterized, typed strain of *M. globosa* was obtained from the fungal culture collection of the Department of Microbiology, Federal Medical Centre Teaching Hospital, Owerri, Nigeria. To ensure viability and optimal propagation, the isolate was aseptically subcultured onto Sabouraud Dextrose Agar (SDA) (Neogen Culture Media, USA) supplemented with 0.05 % chloramphenicol (~98 %, CDH Fine Chemicals, India) to inhibit bacterial contamination. Given the lipophilic nature of *Malassezia* species, the surface of each plate was overlaid with 2–3 drops of sterile olive oil, serving as an exogenous lipid source essential for fungal growth.[16] The inoculated plates were incubated at 32 °C for 14 days under aerobic conditions to facilitate colony development and sporulation. Successful growth was confirmed through characteristic colony morphology, and the propagated cultures were subsequently used for antifungal susceptibility testing. This protocol ensured the maintenance of fungal purity, viability, and phenotypic stability throughout the study.

Plant extract preparation

Fresh red and green leaves of *A. wilkesiana* (Figure 1) were collected in May 2025 from a verified botanical source along Okigwe Road, Owerri, Imo State (Latitude 5.498976° N; Longitude 7.034896° E), and authenticated by Prof. F.N. Mbagwu, a professional taxonomist in the Department of Plant Science and Biotechnology, Imo State University, Owerri.

Figure 1: Green and red variety of *A. wikesiana* used in the study

Voucher specimens were deposited at the Imo State University Herbarium, with deposition identities IMSUH 486 and IMSUH 487 for the red and green varieties, respectively. The fresh leaves were rinsed with deionized water and air-dried on sterile cotton cloth at room temperature. The leaves were homogenized into a fine paste using a sterilized porcelain mortar and pestle. Exactly 5 g of each paste was cold-macerated in 50 mL of 70 % ethanol (≥99.8 %, Honeywell, USA) for 24 h in amber-colored containers. After filtration with Whatman No. 1 paper, the extracts were concentrated at 40 °C under reduced pressure using a rotary evaporator (Rotavapor R-80, BUCHI Labortechnik AG, Switzerland), yielding semi-solid crude ethanolic extracts.[17] These were stored in sterile vials at 4 °C until further analyses. This standardized protocol preserved heat-sensitive bioactives and ensured reproducibility.

Preparation of inoculum and antifungal susceptibility testing

The antifungal assay was performed using a standardized protocol,[18] with slight modifications. An inoculum of *M. globosa* was prepared by transferring growth from a fresh isolate into 4 mL of 0.85 % NaCl using a flame-sterilized loop. The suspension was vortexed and adjusted to the 0.5 McFarland standard to ensure uniform density.

Within 15 min, 0.1 mL of inoculum was spread onto SDA plates supplemented with 0.05 % chloramphenicol and 2–3 drops of sterile olive oil to support *Malassezia* growth. Plates were prepared in triplicate. As a positive control, an Oxoid™ ketoconazole disc (10 µg; Thermo Fisher Scientific, UK) was placed at the center of each plate. For test samples, sterile paper discs soaked with 50 µL of crude ethanolic extracts from either the green or red *A. wilkesiana* variants were aseptically placed on the agar surface. After a 15 min pre-diffusion at room temperature, the plates were incubated at 32 °C for 14 days. Zones of inhibition were then measured to compare extract activity with that of the standard antifungal agent.

Phytochemical profiling by gas chromatography-mass spectrometry (GC-MS)

The phytochemical profile of ethanolic extracts from red and green *A. wilkesiana* leaves was analyzed by Gas Chromatography-Mass Spectrometry (GC-MS) (Agilent Technologies, 7890 GC and 5977B Mass Selective Detector (MSD)). Approximately 1 µL of each concentrated extract was injected in splitless mode, with helium as the carrier gas at a flow rate of 1.0 mL/min. Separation was achieved on an HP-5MS capillary column (30 m × 0.25 mm, 0.25 µm film thickness). The oven was programmed from 60 °C (2 min hold) to 280 °C at 10 °C/min, followed by a final hold at 280 °C for 10 min. Injector and detector temperatures were maintained at 250 °C and 280 °C, respectively. The mass spectrometer was set to scan from m/z 40–500 to capture low- to medium-molecular-weight constituents. Resulting spectra were processed against the NIST Mass Spectral Library using integrated search software for tentative compound identification based on similarity scores. This approach provided a comprehensive chemical characterization of the extracts, forming the basis for subsequent in-silico and biological evaluations.[19]

Ligand and target preparation, and molecular docking studies

The three-dimensional (3D) molecular structures of phytochemicals identified in the crude ethanolic extracts of the red and green varieties of *A. wilkesiana*, as determined by GC–MS analysis, were retrieved in Structure Data Format (SDF) from the PubChem compound database (https://pubchem.ncbi.nlm.nih.gov). These structures were subjected to geometry optimization using Open Babel, integrated in Python Prescription software (Open Babel Development Team, version 0.8, 2005), employing the Merck Molecular Force Field 94 (MMFF94) to obtain energetically favorable conformations. The target macromolecule, mono- and diacylglycerol lipase from *M. globosa* (Figure 2), designated as SMG1 and available under PDB ID: 3UUE, was retrieved from the Protein Data Bank (https://www.rcsb.org/structure/3UUE).

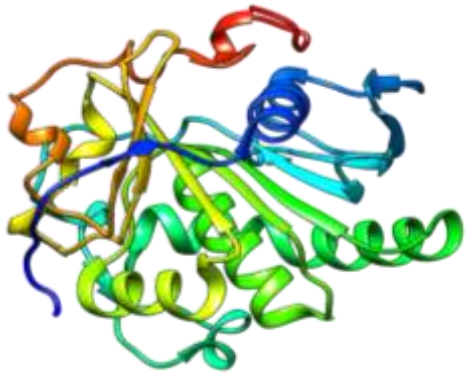

Figure 2: Crystal structure of mono- and diacylglycerol lipase from *M. globosa*

The protein structure was prepared for docking simulations by removing water molecules, heteroatoms, and co-crystallized ligands, followed by energy minimization using Cresset Flare© (Cresset Cambridge, UK, version 4.0, 2020). The General Amber Force Field (GAFF) was applied, with minimization parameters set to a gradient cutoff of 0.200 kcal/mol/Å and a maximum of 2000 iterations, to stabilize the protein geometry.

Molecular docking was conducted using a flexible docking protocol, [20] implemented in AutoDock Vina (Scripps Research, version 1.2.0, 2021). The active site was defined using a grid box with dimensions of 17.138 × 13.292 × 9.279 Å, centered on the binding pocket of the SMG1 enzyme. Docking simulations generated multiple binding poses for each ligand, with associated binding affinity scores (kcal/mol). The most energetically favorable complexes were selected based on their lowest binding energy and were subsequently visualized and analyzed for key molecular interactions.

Molecular dynamics simulation of protein-ligand complex

To complement the static binding predictions from molecular docking and to assess the dynamic behavior and structural stability of the ligand–receptor complex under physiologically relevant conditions, all-atom molecular dynamics (MD) simulations were performed. The lead phytochemical compound, identified from docking studies as having the strongest binding affinity to the mono- and diacylglycerol lipase of *M. globosa*

(SMG1), was used as the initial structure for a 100-nanosecond (ns) simulation using the Desmond simulation package of Schrödinger LLC (Schrödinger Release, 2017-3), following standard protocols.[21] The initial complex was preprocessed using the Protein Preparation Wizard, which involved the assignment of bond orders, addition of hydrogen atoms, optimization of the hydrogen-bonding network, and restrained energy minimization. The System Builder module was used to embed the complex in an orthorhombic periodic boundary box, with solvation achieved using SPC (Simple Point Charge) water molecules and the OPLS (Optimized Potentials for Liquid Simulations) all-atom force field.

The system was neutralized by the addition of counterions, and 0.15 M NaCl was added to simulate physiological ionic strength. The simulation was conducted under isothermal–isobaric (NPT) ensemble conditions at a constant temperature of 300 K and pressure of 1 atm, maintained using the Berendsen thermostat and barostat algorithms, respectively. Prior to the production run, the system underwent energy minimization and equilibration steps. During the simulation, trajectory snapshots were recorded every 10 picoseconds (ps) for subsequent analyses. The root-mean-square deviation (RMSD) of the protein–ligand complex backbone atoms was calculated over the course of the simulation to evaluate the structural integrity and binding stability of the ligand within the SMG1 active site.

In-silico toxicity profiling of lead compound

The potential toxicity profile of the lead compound, particularly in relation to dermal and systemic safety, was comprehensively evaluated using advanced in-silico predictive platforms. A comparative analysis with ketoconazole, a standard antifungal agent, was conducted using three web-based tools: pkCSM [22], ADMET-AI [23], and ADMETlab 3.0 [24]. These platforms leverage robust machine learning algorithms and extensive chemical–biological datasets to forecast a variety of toxicological endpoints. The compounds were submitted in their canonical SMILES format, and each tool independently applied predictive modeling, ranging from graph-based signatures and neural networks to ensemble learning methods, to generate toxicity scores.

Quantum chemical calculations via density functional theory (DFT)

Density Functional Theory (DFT) calculations were performed to investigate the molecular geometry, electronic distribution, and reactivity indices of the lead *A. wilkesiana* phytochemical in comparison with ketoconazole and the native co-crystallized ligand. All computations were carried out using Gaussian 09W (Gaussian Inc., 2010) with the B3LYP functional and the 6-311++G(2d,2p) basis set. Molecular geometries were fully optimized without symmetry constraints, and frontier molecular orbitals (HOMO and LUMO) were analyzed to evaluate electronic reactivity and stability. The HOMO–LUMO energy gap (Equation 1) was used as a descriptor of electronic hardness and polarizability.[25] Molecular visualizations, including optimized structures and HOMO–LUMO surfaces, were generated with GaussView 6.0 (Gaussian Inc., 2018). These computations provided mechanistic insights into electronic behavior and interaction propensities, supporting rational drug design and docking validation.

$$E_{gap} = E_{LUMO} - E_{HOMO} \quad (1)$$

Statistical analysis

All experimental data were generated in triplicates and expressed as mean ± standard deviation (SD). Differences between treatment groups (red and green leaf extracts, positive control, and untreated control) were analyzed using one-way analysis of variance (ANOVA), followed by Tukey's post-hoc multiple comparison test to determine statistical significance. A p-value < 0.05 was considered statistically significant. GraphPad Prism 8.0.1 (GraphPad Software, San Diego, CA, USA) was used for all statistical computations.

RESULT AND DISCUSSION

In-vitro* antifungal activity of *A. wikesiana* leaf extracts against *M. globosa

The in-vitro antifungal assay (Figure 3) demonstrated a markedly superior inhibitory effect of the crude ethanolic extract derived from the red variety of *A. wikesiana*, as evidenced by a zone of inhibition measuring 60 mm, which significantly surpassed that of the standard antifungal agent, ketoconazole (35 mm), under identical experimental conditions. In contrast, the crude extract from the green variant of *A. wikesiana* exhibited no observable inhibitory activity, with the *M. globosa* isolate demonstrating resistance, thereby reinforcing variant-dependent bioactivity. These results are consistent with earlier reports, [14, 26] which similarly documented strong antifungal activity associated with the red variant of *A. wikesiana*. The pronounced antifungal potency observed in the red variant may be attributed to the presence of specific bioactive secondary metabolites with lipase-inhibitory properties,

particularly effective against lipid-dependent dermatophytes such as *M. globosa*.

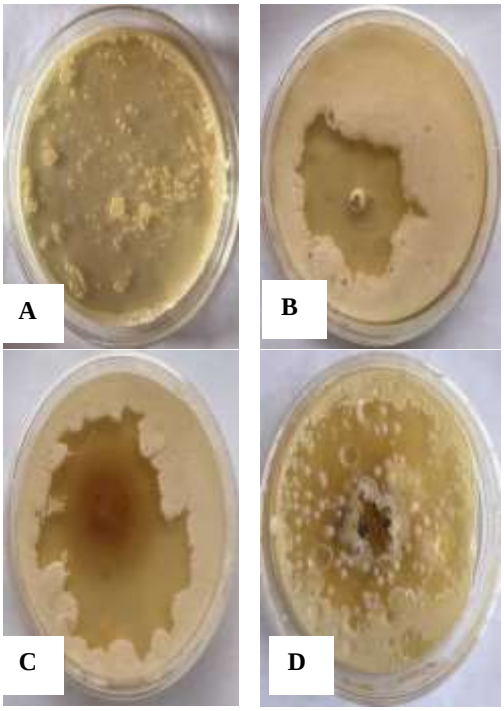

Phytochemical profiling of A. wikesiana leaf extracts using GC-MS analysis

Gas Chromatography–Mass Spectrometry (GC-MS) analysis was employed to comprehensively elucidate the phytochemical constituents present in the ethanolic crude extracts of both green and red variants of *A. wikesiana*. The chromatographic profiles obtained (Figure 4) provided detailed separation and identification of compounds based on their unique retention times and mass-to-charge (m/z) ratios, thereby facilitating a qualitative and semi-quantitative assessment of the chemical diversity within the extracts. Comparative analysis revealed a significantly higher abundance and diversity of phytochemicals in the red variant relative to the green counterpart (Table 1). Notably, fatty acid methyl esters (FAMEs) emerged as the dominant class of compounds in both variants, underscoring their lipophilic character and potential bioactivity against lipid-dependent microorganisms. In the green variant, decane, 3,8-dimethyl- (41.02 %) and oleic acid, methyl ester (17.35 %) were the most abundant constituents, while the red variant was characterized by a prominent presence of oleic acid, methyl ester (28.20 %) and 1-heptadecene (20.32 %).

These compositional differences suggest a chemotypic variation between the two variants, which may underlie the observed disparities in their biological activity. The enriched profile of bioactive phytochemicals in the red variant, particularly unsaturated fatty acids and alkenes, provides a plausible biochemical basis for its superior antifungal efficacy.

Molecular docking analysis of A. wikesiana phytochemicals targeting M. globosa lipase

To elucidate the antifungal potential of phytochemicals derived from the red and green variants of *A. wikesiana*, molecular docking simulations were performed against mono- and diacylglycerol lipase from *M. globosa*. This computational approach enabled the investigation of non-covalent interactions at the molecular level, providing insights into ligand–receptor binding mechanisms and the thermodynamic stability of the resulting complexes.[27-28] The docking simulations, validated by the inclusion of Ketoconazole, a clinically established antifungal agent effective against *Malassezia* species [29] served as a benchmark to assess the relative efficacy of the plant-derived compounds.

Docking scores, expressed as binding free energy (kcal/mol), revealed that phytochemicals from the green variant demonstrated significantly lower binding affinities than both Ketoconazole and the native ligand, indicating limited lipase-inhibitory activity. Conversely, compounds isolated from the red variant, notably aspidospermidin-17-ol, 1-acetyl-19,21-epoxy-15,16-dimethoxy- (ASP), exhibited a superior binding affinity of –6.8 kcal/mol, surpassing both Ketoconazole and the co-crystallized ligand (–6.4 kcal/mol). Another compound, cis-vaccenic acid, also showed moderate activity with a binding energy of –6.0 kcal/mol. These in-silico findings corroborate the results of the in-vitro antifungal assays, positioning ASP as a promising lipase inhibitor and potential antifungal lead compound. Although ASP has been previously identified in various plant sources,[30-31] its pharmacological profile remains largely unexplored. This study is the first to propose its potential antifungal utility, laying the groundwork for subsequent experimental validation and mechanistic exploration.

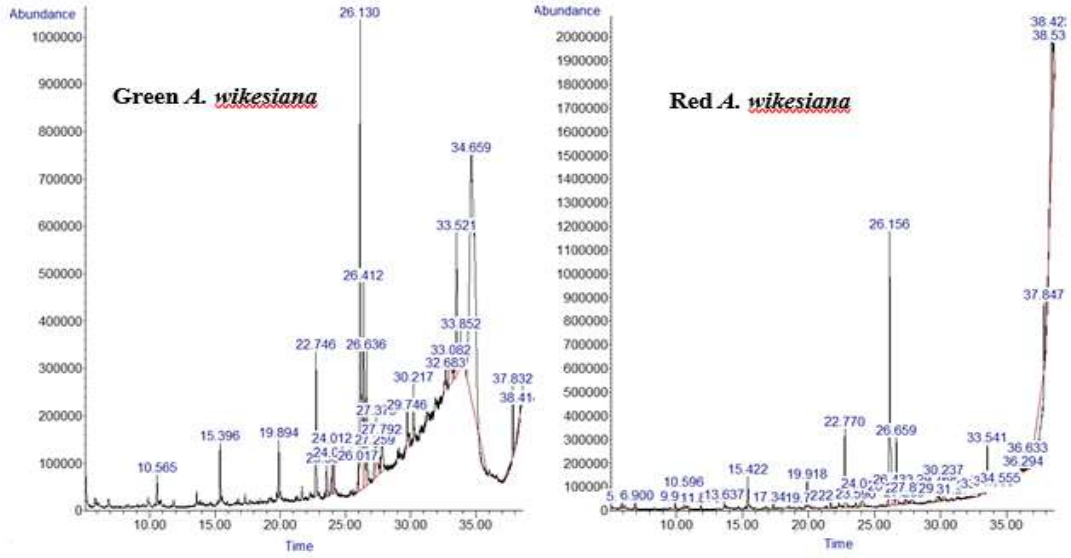

Figure 4: GC-MS chromatogram of the crude extract from green and red *A. wikesiana*

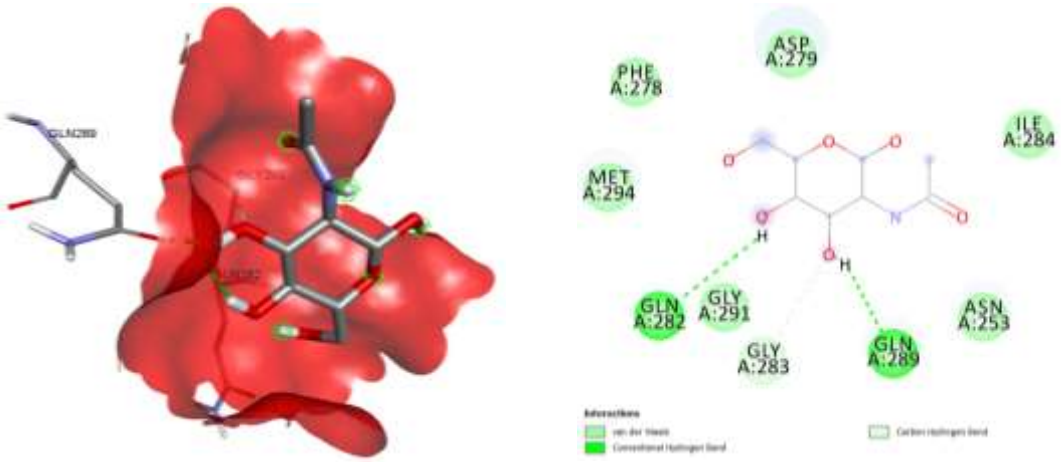

N-acetyl D-glucosamine

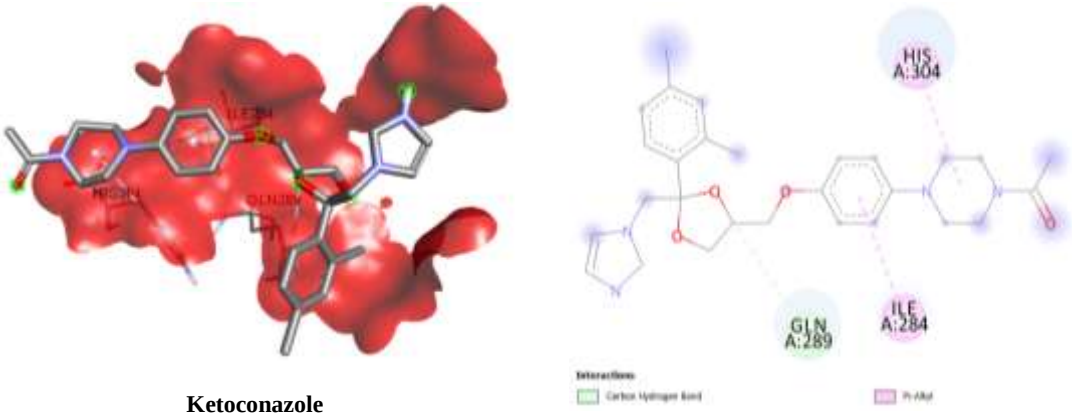

Ketoconazole

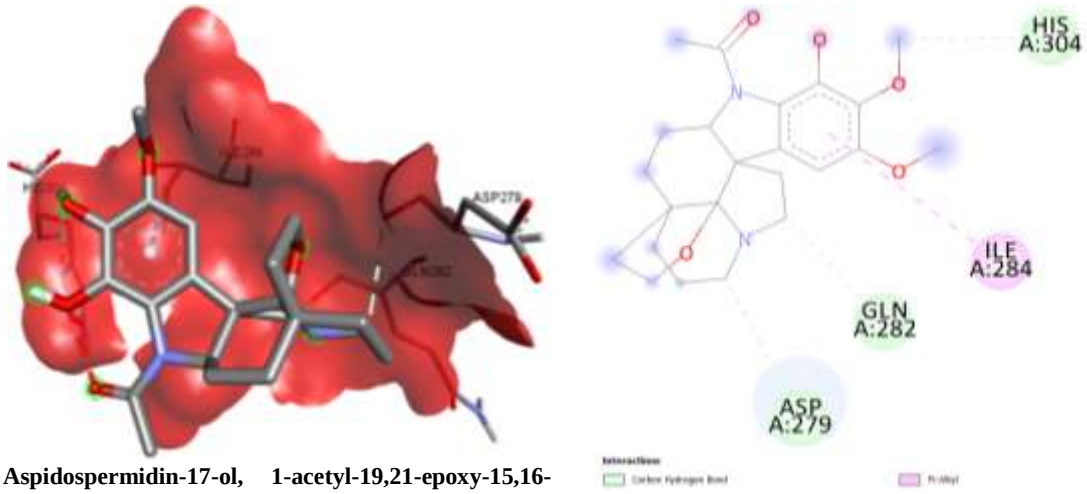

Aspidospermidin-17-ol, 1-acetyl-19,21-epoxy-15,16-dimethoxy-

Figure 5: 3D and 2D views of ligand-amino acid interactions at the *M. globosa* lipase active site

Table 1: Phytochemicals in green and red *A. wikesiana* variants and their binding affinities at the *M. globosa* lipase target

Percentage	Compound	PubChem CID	Binding energy (kcal/mol)
	Green *A. wikesiana* variety		
41.02	Decane, 3,8-dimethyl-	519396	– 3.9
17.35	Oleic acid, methyl ester	5364509	– 4.6
7.37	Phytol	5280435	– 4.7
5.28	Methyl 20-methyl-heneicosanoate	15089804	– 4.2
4.22	Stearic acid, methyl ester	8201	– 4.5
4.02	Pentadecanoic acid, 14-methyl-, methyl ester	21205	– 4.5
2.88	1,5-cyclodecadiene, (E,Z)-	5365643	– 4.5
2.57	Oleic acid	445639	– 4.8
2.14	3-eicosene, (E)-	5365051	– 4.3
1.92	10-heneicosene (c,t)	5364553	– 4.5
1.91	Methyl 10-methyl-hexadecanoate	10401643	– 4.2
1.47	2-Tetradecene, (E)-	5352912	– 4.1
1.42	9-eicosene, (E)-	5365037	– 4.3
1.42	1-docosene	74138	– 4.0
1.21	Palmitic acid, ethyl ester	12366	– 4.7
1.12	Dibutyl phthalate	3026	– 4.6
0.98	Linoleic acid, methyl ester	5284421	– 4.3
0.91	3-tetradecene, (Z)-	5362709	– 4.0
0.65	Squalene	638072	– 4.1
0.41	3-Chloropropionic acid, heptadecyl ester	545757	– 4.4
0.10	Cyclopropaneoctanal, 2-octyl-	550143	– 4.4
	Red *A. wikesiana* variety		
28.20	Oleic acid, methyl ester	5364509	– 4.6
20.32	1-heptadecene	23217	– 4.5
6.78	2-chloropropionic acid, octadecyl ester	522892	– 4.4
6.04	Palmitic acid, methyl ester	12366	– 4.7
5.73	Stearic acid, methyl ester	8201	– 4.5
4.64	Docosanoic acid, methyl ester	13584	– 4.5
3.60	Oleic acid	445639	– 4.8

	3.48	9-octadecene, (E)-	5364599	– 4.3
	2.60	Phytol	5280435	– 4.7
	1.96	Methyl 18-methylnonadecanoate	530340	– 4.7
	1.32	8,11-octadecadienoic acid, methyl ester	5319737	– 4.9
	1.32	cis-vaccenic acid	5282761	– 6.0
	1.26	Z-8-hexadecene	5352971	– 4.0
	1.07	Trifluoroacetoxy hexadecane	522035	– 4.4
	0.94	Aspidospermidin-17-ol, 1-acetyl-19,21-epoxy-15,16-dimethoxy-	550059	**– 6.8**
	0.89	Phthalic acid, isobutyl octadecyl ester	6423451	– 4.6
	0.87	cis-11-eicosenoic acid	5282768	– 4.6
	0.87	Pentadecafluorooctanoic acid, octadecyl ester	15918848	– 3.1
	0.74	Oxirane, [(hexadecyloxy)methyl]-	61823	– 4.0
	0.71	Dichloroacetic acid, heptadecyl ester	546049	– 4.1
	0.69	Cyclohexane, hexyl-	20283	– 4.6
	0.68	13-Octadecenal, (Z)-	5364497	– 4.3
	0.66	Oxiraneundecanoic acid, 3-pentyl-, methyl ester, trans-	91692401	– 4.6
	0.64	Chloroacetic acid, 4-tetradecyl ester	536959	– 4.5
	0.53	Cyclohexane, octyl-	15712	– 4.0
	0.50	1-tridecene	17095	– 3.7
	0.48	Propyl tetracosyl ether	91409396	– 3.7
	0.47	8-Pentadecanone	13162	– 4.3
	0.46	Butylated hydroxytoluene	31404	– 4.7
	0.33	9-Oxabicyclo[6.1.0]nonane	67513	– 4.2
	0.31	1-dodecene	8183	– 3.6
	0.20	1-Hexene, 4-ethyl-	123365	– 3.8
	0.15	Heptadecanoic acid, heptadecyl ester	545561	– 4.3
	0.56	Squalene	638072	– 4.1
Native ligand		N-acetyl D-glucosamine	24139	**– 6.4**
Drug		Ketoconazole	456201	**– 6.4**

Figure 5 illustrates the molecular interactions between the native ligand of the lipase, Ketoconazole, and the identified lead compound (ASP) with the amino acids at the enzyme's active site, providing a detailed visual representation of the binding modes and interactions of these ligands with the target enzyme. The binding of the native ligand to the lipase active site was mediated by conventional hydrogen bonds, van der Waals interactions, and carbon-hydrogen interaction. In contrast, Ketoconazole and ASP exhibited distinct binding modes, engaging the active site through pi-alkyl and carbon-hydrogen bond interactions. Notably, the residues HIS304 and ILE284 played a crucial role in the formation of the enzyme-ligand complex with both Ketoconazole and ASP, suggesting a shared mechanism of inhibition for these two compounds against *M. globosa* lipase.

Molecular dynamics simulation of the SMG1–ASP complex

To assess the dynamic stability of the protein–ligand interaction, a 100-nanosecond (ns) all-atom MD simulation was conducted on the lead compound, ASP, in complex with mono- and diacylglycerol lipase from *M. globosa* (SMG1). The simulation aimed to evaluate the conformational integrity and stability of the ASP–lipase complex under physiological conditions by monitoring the root mean square deviation (RMSD) of the protein backbone over the simulation trajectory. Typically, RMSD values ranging from 1 to 4 Å are indicative of a stable protein–ligand interaction, whereas values exceeding 4 Å often signal substantial structural rearrangements.[32]

The RMSD trajectory (Figure 6) revealed that the unbound SMG1 receptor (apo form) exhibited moderate fluctuations, averaging approximately 2.5 Å, with noticeable deviations occurring around

25 ns and 65 ns. In stark contrast, the SMG1–ASP complex demonstrated superior structural stability, with the ligand-bound system attaining rapid equilibrium and maintaining an average RMSD of 0.8Å throughout the entire 100 ns simulation period.

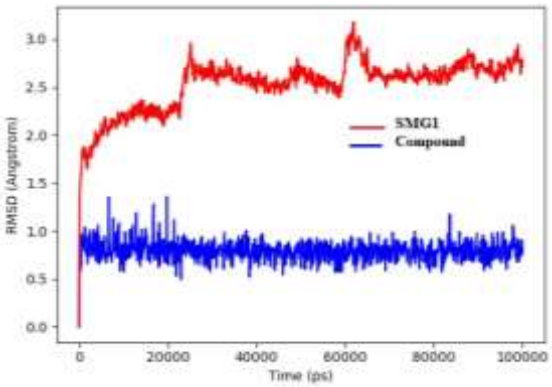

Figure 6: RMSD Plot for SMG1 and SMG1-ASP Complex at 100 ns

This low degree of fluctuation signifies a rigid and well-maintained binding conformation, thereby affirming the strong binding affinity observed in the docking studies. Collectively, these results underscore the dynamic stability of the SMG1–ASP complex and reinforce the potential of ASP as a robust antifungal agent for the therapeutic management of SD.

Toxicity properties for skin sensitivity of lead compound

The potential toxicity and side effects of the lead compound were assessed using toxicity web servers. Skin permeability, a critical parameter in evaluating transdermal delivery, was analyzed, with values ranging from –8.0 to –1.0 considered standard.[33] This parameter quantitatively describes the rate of penetration across the stratum corneum and the transport of molecules in the outermost layer of the epidermis. A lower log K_p value indicates reduced permeability of the molecule through the skin.[34]

The comparative toxicity analysis between Ketoconazole, a conventional antifungal agent, and ASP, the lead phytochemical from *A. wilkesiana* (Table 2), revealed insightful implications regarding the latter's potential as a safer topical antifungal alternative. Water solubility, expressed as log S, was slightly lower for ASP (–3.905) than for Ketoconazole (–3.668), indicating marginally reduced aqueous solubility. While this may influence formulation considerations, it remains within acceptable limits for topical administration. Skin permeability (log K_p), another critical parameter for dermal delivery, was more negative for ASP (–3.453 cm/s) compared to Ketoconazole (–2.735 cm/s), suggesting that ASP may have lower transdermal penetration. This reduced permeability could limit systemic absorption and associated side effects, representing an advantageous feature for localized therapy.

Table 2: Comparison of the toxicity properties of ASP and Ketoconazole

Toxicity parameters	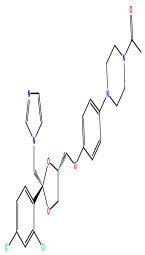 **Ketoconazole**	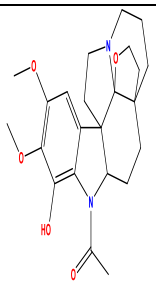 **ASP**
Water solubility (log S)	– 3.668	– 3.905
Skin permeability log K_p (cm/s)	– 2.735	– 3.453
Skin sensitization	No	No
Skin reaction	0.28	0.14
Hematotoxicity	0.66	0.43
Carcinogenicity	0.14	0.01

Both compounds were predicted to be non-sensitizing to the skin, reinforcing their dermatological safety. Importantly, ASP exhibited significantly lower skin reaction and hematotoxicity scores (0.14 and 0.43, respectively) than Ketoconazole (0.28 and 0.66), indicating a reduced risk of inflammatory and systemic hematologic effects. Most notably, the carcinogenicity probability for ASP (0.01) was markedly lower than that of Ketoconazole (0.14), underscoring ASP's superior long-term safety profile.

Frontier molecular orbital analysis and reactivity implications

The frontier molecular orbital energies, particularly the HOMO and LUMO, serve as critical parameters for evaluating the electronic and chemical reactivity of drug-like molecules. The HOMO functions as the primary electron donor, whereas the LUMO serves as the primary electron acceptor in molecular interactions, thus providing valuable insights into charge-transfer mechanisms and reactivity at the active site.[35] The

energy difference between these orbitals, known as the HOMO–LUMO energy gap (E_{gap}), is indicative of a compound's chemical stability and reactivity; a smaller gap generally correlates with higher reactivity and reduced kinetic stability.[36]

As presented in Table 3, the calculated molecular orbital energy values for the native ligand, Ketoconazole, and the lead compound ASP reveal that Ketoconazole possesses the smallest energy gap, signifying the highest potential reactivity among the three compounds. Notably, ASP exhibits a comparable energy gap, slightly higher than Ketoconazole but significantly smaller than that of the native ligand. This close proximity in energy values implies that ASP may demonstrate a similar degree of chemical reactivity and binding potential at the target site as Ketoconazole, thereby reinforcing its promise as a viable antifungal candidate. Furthermore, the lower energy gap of ASP compared to the native ligand highlights its superior potential for electronic interactions, which could translate into enhanced biological efficacy against the lipase target of *M. globosa*. These findings support the continued exploration of ASP as a structurally novel and electronically favorable lead compound for antifungal drug development.

Table 3: Molecular orbital energy values for the controls and lead molecule

Parameter	**Compounds**		
	ASP	***N-acetyl D-glucosamine***	***Ketoconazole***
Optimized structure		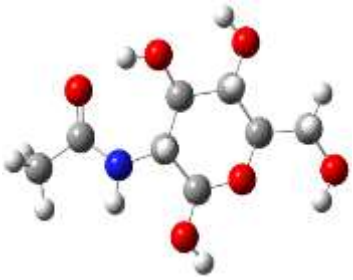	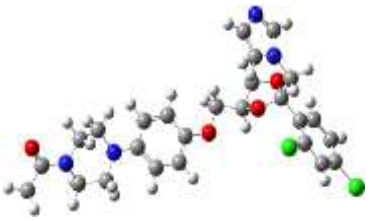
LUMO (eV)	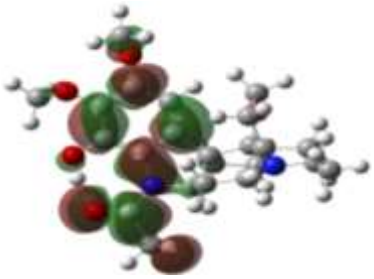 $E_{LUMO} = -0.6514$	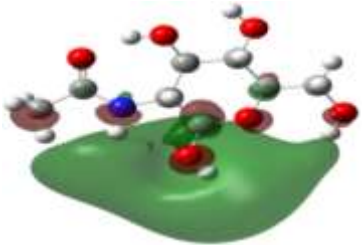 $E_{LUMO} = -0.7861$	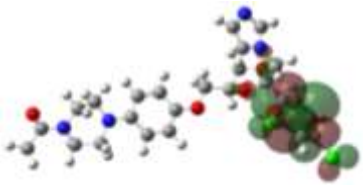 $E_{LUMO} = -1.3706$
HOMO (eV)	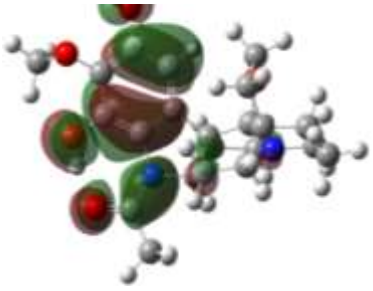 $E_{HOMO} = -5.7514$	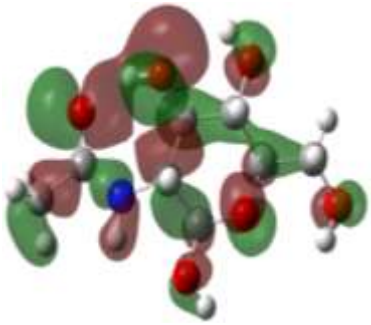 $E_{HOMO} = -7.5692$	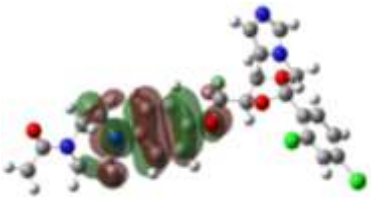 $E_{HOMO} = -5.2665$
Energy gap (eV)	5.100	6.783	3.896

CONCLUSION

This study demonstrates that phytochemicals from the red variant of *Acalypha wilkesiana* possess notable antifungal activity against *Malassezia globosa*, primarily through inhibition of its lipase enzyme, a key virulence factor in seborrheic dermatitis. Among the compounds identified, aspidospermidin-17-ol, 1-acetyl-19,21-epoxy-15,16-dimethoxy-, exhibited superior binding affinity, stability, and safety profiles, outperforming the standard antifungal agent ketoconazole *in-silico*. The integration of GC–MS profiling, molecular docking, molecular dynamics simulations, and quantum chemical analysis underscores the robustness of this multidimensional approach in natural product-based drug discovery. These findings validate the ethnomedicinal relevance of *A. wilkesiana* and highlight its potential as a source of novel antifungal candidates for topical applications. Future studies should prioritize the isolation and structural elucidation of lead compounds, coupled with *in-vitro* lipase inhibition and cytotoxicity assays, to rigorously validate their bioactivity and establish preliminary safety profiles. *In-vivo* studies in dermatitis models should further confirm therapeutic efficacy, while formulation development, particularly topical gels or ointments can enable practical delivery. Integrating QSAR modeling, SAR analysis, and pharmacokinetic studies will aid in optimizing potency and safety, thereby paving the way for preclinical and clinical evaluations. These efforts could position *A. wilkesiana*-derived compounds as safer, plant-based antifungal alternatives to conventional therapies in the face of rising resistance.

CONFLICT OF INTEREST

The authors declare no conflict of interest.

AUTHORS DECLARATION

The authors hereby declare that the works presented in this article are original and that any liability for claims relating to the content of this article will be borne by them.

Funding

This project was sponsored by The Tertiary Education Trust Fund (TETFund) under the TETFund reference number TETF/DR&D/CE/UNI/OWERRI/IBR/2025/VOL. 1

REFERENCES

1. Dall'Oglio F, Nasca MR, Gergino C, Micali G. An overview of diagnosis and management of seborrheic dermatitis. Clin Cosmet Investig Dermatol. 2020;15:1537-1848.
2. Schoch JJ, Monin RL, Satcher KG, Harris J, Triplett E, New J. The infantile cutaneous microbiome: a review. Pediatr Dermatol. 2019;36(5):574-580.
3. Araya M, Kutthanan K, Jiamton S. Clinical characteristics and quality of life of seborrheic dermatitis patients in a tropical country. Indian J Dermatol. 2015;60(5):5-19.
4. Rhimi W, Theeler B, Boekhout T, Otranto D, Catarchia C. Malassezia spp.: yeasts of emerging concern in fungemia. Front Cell Infect Microbiol. 2020;10:370.
5. Park M, Park S, Jung WH. Skin commensal fungus Malassezia and its lipases. J Microbiol Biotechnol. 2021;31(5):637-644.
6. Sparber F, De Gregorio C, Steckholzer S, Cilata M, Salluto F, Gut-Landmann SL. The skin commensal yeast Malassezia triggers a type 17 response that coordinates antifungal immunity and exacerbates skin inflammation. Cell Host Microbe. 2019;25:389-403.
7. Park M, Park S, Jung WH. Skin commensal fungus Malassezia and its lipases. J Microbiol Biotechnol. 2021;31(5):637-644.
8. Adalsteinsson JA, Kaushik S, Muzumdar S, Guttman-Yassky E, Ungar J. An update on the microbiology, immunology and genetics of seborrheic dermatitis. Exp Dermatol. 2020;29:481-489.
9. Mustarichie R, Rostinawati T, Pitaloka DAE, Saptarini NM, Iskandar Y. Herbal therapy for the treatment of seborrheic

dermatitis. Clin Cosmet Investig Dermatol. 2022;15:2391-2405.

10. Sulaiman AN, James AE. Phytochemical constituents and antifungal activity of *Acalypha wilkesiana* leaves on *Candida albicans*. J Sci. 2023;7(3):209-214.
11. Madziga HA, Chiromo M, Sanni S, Sandabe UK, Sodipo OA. Effects of aqueous leaf extract of *Acalypha wilkesiana* on some serum biochemical profiles of mice in acute toxicity studies. Sahel J Vet Sci. 2020;17(3):1-5.
12. Sherifat KO, Itohan AM, Adeola SO, Adeola KM, Aderemi OL. Antifungal activity of *Acalypha wilkesiana*: a preliminary study of fungal isolates of clinical significance. Afr J Infect Dis. 2022;16(1):21-30.
13. Isaac AO, Tolupe AC. Phytochemical and antifungal screening of *Acalypha wilkesiana* Mull Arg (Euphorbiaceae) leaf extract in cream formulations. Niger J Pharm Appl Sci Res. 2022;5(1):36-41.
14. Katibi OS, Aboh MI, Sclawu OA, Kola-Mustapha A, Olatunyi LA. Antifungal activity of Acalypha wilkesiana: a preliminary study of fungal isolates of clinical significance. Afr J Infect Dis. 2022;16(1):21-30.
15. Uloma UUN, Ilomuanya MO, Salem AI, Mercy A, Oludolapo K, Chukwuemeka AP, Oluwakayinsola S. Evaluation of the antimicrobial effectiveness of topical gels containing Acalypha wilkesiana. Trop J Nat Prod Res. 2021;5(8):1470-1477.
16. Romald PN, Kindo AJ, Mahalakshmi V, Umadevi U. Epidemiological pattern of Malassezia, its phenotypic identification and antifungal susceptibility profile to azoles by broth microdilution method. Indian J Med Microbiol. 2020;38(3-4):351-356.
17. Ikezu UM, Duru CE, Ikpa CB, Ibe FC. In silico discovery of dual-targeting molecules from *Acalypha wilkesiana* against hypertension and hyperglycemia. Discov Chem. 2025;2:86.
18. Zaputa A, Acros SR. A comparative study of McFarland turbidity standards and the Densimat photometer to determine bacterial cell density. Curr Microbiol. 2015;70:907-909.
19. Enenebeaku UE, Duru CE, Mgbemena IC, Ukwandu NCD, Nwigwe HC, Enenebeaku CK, Okotcha EN. Phytochemical evaluation and molecular docking of bioactive compounds from the roots of *Dictyandra arborescens* (Welw.) against *Plasmodium berghei* protein targets. Trop J Nat Prod Res. 2021;5(2):370-381.
20. Duru IA, Duru CE. Molecular docking of compounds in the essential oil of Ocimum gratissimum leaf against PIM-1 kinase of Escherichia coli. Eur J Adv Chem Res. 2020;1(6):1-4.
21. Ivanova L, Tammiku-Taul J, García-Sosa AT, Sidorova Y, Saarma M, Karelson M. Molecular dynamics simulations of the interactions between glial cell line-derived neurotrophic factor family receptor GFRα1 and small-molecule ligands. ACS Omega. 2018;3(9):11407-11414.
22. Pires DEV, Blundell TL, Ascher DB. pkCSM: predicting small-molecule pharmacokinetic properties using graph-based signatures. J Med Chem. 2015;58(9):4066-4072.
23. Swanson K, Walther P, Leitz J, Mukherjee S, Wu JC, Shivnaraine RV, Zou J. ADMET-AI: a machine learning ADMET platform for evaluation of large-scale chemical libraries. bioRxiv. 2023; Dec 28.
24. Duan Y, Yang X, Zeng X, Wang W, Deng Y, Cao D. Enhancing molecular property prediction through task-oriented transfer learning: integrating universal structural insights and domain-specific knowledge. J Med Chem. 2024;67(11):9575-9586.
25. Duru CE, Chidiebere CW. Computer-assisted discovery of tyrosinase inhibitors from turmeric and clove: an in silico study on natural skin-whitening agents and their potential toxicity. S Afr J Bot. 2024;175:669-683.
26. Sherifat KO, Itohan AM, Adeola SO, Adeola KM, Aderemi OL. Antifungal activity of *Acalypha wilkesiana*: a preliminary study of fungal isolates of clinical significance. Afr J Infect Dis. 2021;16(1):21-30.
27. Nwofor CN, Duru CE, Onyenwe NE. Computational identification of small molecules in *Mitracarpus scaber* ethanolic leaf extract with fungal keratinase inhibitory potentials. J Nat Pestic Res. 2022;2:100010.
28. Akanbi AI, Izevbigie EV, Sherif AO, Dlamini NH, Fadele LO, Oyawaluja BO. Molecular docking, ADME and SAR analysis of 383 phytochemicals in the quest for lead antidiabetic inhibitors targeting α-amylase and α-glucosidase

enzymes. Trop J Drug Res. 2025;2(1):6-13.

29. Wang K, Cheng L, Li W, Jiang H, Zhang X, Liu S, Huang Y, Qiang M, Dong T, Li Y, Wang J, Feng S, Li H. Susceptibilities of *Malassezia* strains from pityriasis versicolor, *Malassezia* folliculitis and seborrheic dermatitis to antifungal drugs. Heliyon. 2020;6(6):e04203.
30. Gopu C, Chirumamilla P, Daravath SB, Vankudoth S, Taduri S. GC-MS analysis of bioactive compounds in the plant parts of methanolic extracts of *Momordica cymbalaria* Fenzl. J Med Plants Stud. 2021;9(3):209-218.
31. Naz S, Alam S, Ahmed W, Khan SM, Qayyum A, Sabir M, Naz A, Iqbal A, Bibi Y, Nisa S, Khalifa AS, Gharib AF, El Askary A. Therapeutic potential of selected medicinal plant extracts against multidrug-resistant *Salmonella enterica* serovar Typhi. Saudi J Biol Sci. 2022;29(2):941-954.
32. Abdullah A, Biswas P, Sahabuddin M, Mubasharah A, Khan DA, Hossain A, Roy T, Rafi NMR, Dey D, Hasan MN, Bibi S, Moustafa M, Shati A, Hassan H, Garg R. Molecular dynamics simulation and pharmacoinformatic integrated analysis of bioactive phytochemicals from *Azadirachta indica* (Neem) to treat diabetes mellitus. J Chem. 2023;4170703.
33. Kumari A, Kumar R, Sulabh G, Singh P, Kumar J, Singh VK, Ojha KK. In silico ADMET, molecular docking and molecular simulation-based study of glabridin's natural and semisynthetic derivatives as potential tyrosinase inhibitors. Adv Tradit Med. 2023;23:733-751.
34. Chen CP, Chen CC, Huang CW, Chang YC. Evaluating molecular properties involved in transport of small molecules in stratum corneum: a quantitative structure–activity relationship for skin permeability. Molecules. 2018;23(4):911.
35. Matin MM, Kumer A, Chandro A, Akash S, Chakma U. Rhamnopyranoside pivaloyl esters as black and white fungus inhibitors: molecular docking, dynamics and ADMET analysis. Orbital Electron J Chem. 2024;16:50-61.
36. Duru IA, Duru CE. Molecular modeling and density functional theory calculation of the coordination behaviour of 4,5-dichloroimidazole with Cu(II) ion. Sci Afr. 2020;9:1-7.